CHEMISTRY
A EUROPEAN JOURNAL

DOI: 10.1002/chem.200802518

Secondary Interactions in Phosphane-Functionalized Group 4 Cycloheptatrienyl–Cyclopentadienyl Sandwich Complexes

Susanne Büschel, Ann-Katrin Jungton, Thomas Bannenberg, Sören Randoll, Cristian G. Hrib, Peter G. Jones, and Matthias Tamm*[a]

Abstract: Phosphane-functionalized cycloheptatrienyl–cyclopentadienyl Group 4 metal complexes of the type $[(\eta^7\text{-}C_7H_7)M(\eta^5\text{-}C_5H_4PR_2)]$ (M = Ti (**9**); M = Zr (**10**); M = Hf (**11**); R = Ph (**a**); R = *i*Pr (**b**)) have been prepared by the reduction of $[(\eta^5\text{-}C_5H_4PR_2)TiCl_3]$ or $[(\eta^5\text{-}C_5H_4PR_2)_2MCl_2]$ (M = Zr, Hf) with magnesium in the presence of cycloheptatriene (C_7H_8). In the solid state, the Ti complex **9a** and the complex **11b** are monomeric, whereas **10a**, **10b**, and **11a** form dimers, in which the sandwich units are linked by long Zr–P or Hf–P bonds. Density-functional theory (DFT) calculations indicate that the metal–phosphane interaction is weak, and accordingly, both the Ti complex **9b** and the Zr complex **10b** act as monodentate phosphane ligands upon reaction with $[\{(cod)RhCl\}_2]$ (cod = η^4-1,5-cyclooctadiene). The X-ray crystal structures of [(cod)Rh(**9b**)Cl] (**12**) and [(cod)Rh(**10b**)Cl] (**13**) reveal that only the latter exhibits a secondary intramolecular Cl–metal interaction. The complex $[(\mathbf{10b})_2Pd]$ (**14**) was obtained by reaction of $[(\eta^5\text{-}C_5H_5)Pd(\eta^3\text{-}C_3H_5)]$ with two equivalents of **10b**. The solid-state structure of **14** reveals a T-shaped Pd^0 center with a long Pd–Zr bond of 2.9709(3) Å, which can be interpreted as a weak noncovalent $Pd^0 \rightarrow Zr^{+IV}$ bond, as indicated by the calculated relaxed force constant of 5.68 N m^{-1}.

Keywords: ambiphilic ligands · metal–metal interactions · noncovalent interactions · phosphane ligands · sandwich complexes

Introduction

Since the serendipitous synthesis and discovery of ferrocene,[1] its modification has become an important task in organometallic chemistry.[2] In particular, ferrocenyl mono- and diphosphanes have become firmly established as ancillary ligands for homogeneously catalyzed reactions[3] that are also of industrial relevance.[3e] In stark contrast, the modification of other sandwich complexes is significantly less developed and, for instance, little use has been made of sandwich complexes containing cycloheptatrienyl (Cht) ligands, even though mixed cycloheptatrienyl–cyclopentadienyl (Cht-Cp) complexes of the type $[(\eta^7\text{-}C_7H_7)M(\eta^5\text{-}C_5H_5)]$ (M = Group 4–6 metals) have been known for more than three decades.[4,5] Surprisingly, $[(\eta^7\text{-}C_7H_6PR_2)Ti(\eta^5\text{-}C_5H_5)]$ (**4**) and $[(\eta^7\text{-}C_7H_6PR_2)Ti(\eta^5\text{-}C_5H_4PR_2)]$ (**5**) represent the only phosphane-functionalized Cht-Cp complexes reported to date, and these ligands were obtained by mono- or dilithiation of $[(\eta^7\text{-}C_7H_7)Ti(\eta^5\text{-}C_5H_5)]$ (**1**, troticene) followed by reaction with the corresponding chlorophosphane $ClPR_2$ (Scheme 1).[6,7] Related derivatizations are unknown for the heavier Group 4 congeners trozircene (**2**) and trohafcene (**3**). Unlike **1**,[8] however, these 16-electron sandwich complexes are capable of reaction with monodentate σ-donor/π-acceptor ligands, such as CO, isocyanides, phosphanes, and *N*-heterocyclic carbenes,[5,9–11] and this potential reactivity prompted us to attempt the synthesis of phosphorus-functionalized Zr and Hf Cht-Cp complexes because these sys-

[a] Dipl.-Chem. S. Büschel, Dipl.-Chem. A.-K. Jungton, Dr. T. Bannenberg, Dr. S. Randoll, Dr. C. G. Hrib, Prof. Dr. P. G. Jones, Prof. Dr. M. Tamm
Institut für Anorganische und Analytische Chemie
Technische Universität Carolo-Wilhelmina zu Braunschweig
Hagenring 30, 38106 Braunschweig (Germany)
Fax: (+49) 531-391-5309
E-mail: m.tamm@tu-bs.de

Supporting information for this article is available on the WWW under http://dx.doi.org/10.1002/chem.200802518.

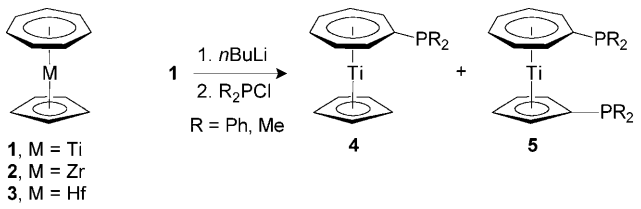

Scheme 1. Synthesis of phosphane-functionalized Cht–Cp complexes.

tems might give rise to interesting secondary interactions involving the Zr or Hf metal atoms.

Results and Discussion

The lithiation of **2** and **3** with *n*BuLi in an analogous manner to that described for **1** proved unsuccessful, and we had to develop an alternative route involving the reduction of zirconocene[12] and hafnocene dichlorides **7** and **8** with magnesium in the presence of cycloheptatriene (C_7H_8; Scheme 2). Filtration and evaporation of the resulting solu-

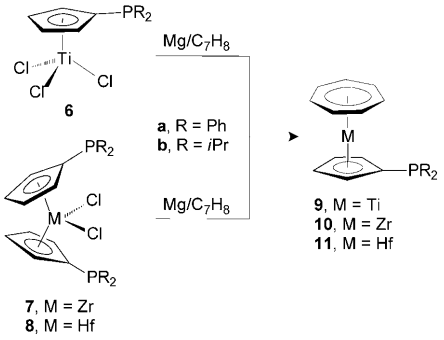

Scheme 2. Synthesis of phosphane-functionalized Cht–Cp complexes.

tions in THF followed by sublimation under high vacuum afforded the Cht–Cp complexes **10** and **11** as orange (**10a**), purple (**10b**), or orange–red (**11a**,**b**) crystalline materials. For comparison, the troticene derivatives **9** were also prepared in a similar manner from $[(\eta^5\text{-}C_5H_4PR_2)TiCl_3]$[13] (**6**), Mg, and C_7H_8. It should be noted that functionalization of the Cp ring alone has never before been achieved for troticene (**1**) and that the PPh_2 derivative **9a** constitutes a structural isomer of the monophosphane **4** (Scheme 1) that was previously obtained through lithiation of the seven-membered ring.[6]

In the ^{31}P NMR spectra, all the complexes give rise to one signal in the expected range, with the signals for the phenyl derivatives **9a**–**11a** ($\delta = -21.7$ to -17.5 ppm) appearing upfield from the signals observed for the isopropyl derivatives **9b**–**11b** ($\delta = 0.0$–3.3 ppm). The latter complexes exhibit two 1:1:1:1 doublets of doublets in their ^1H NMR spectra, in agreement with the presence of diastereotopic *i*Pr methyl groups featuring $^3J_{HH}$ and $^3J_{HP}$ couplings. Accordingly, septets of doublets are observed for the corresponding *i*Pr CH groups. In addition, all complexes show one singlet around $\delta = 5$ ppm for the C_7H_7 hydrogen atoms, whereas more complex AA′BB′ splitting patterns are observed for the four Cp hydrogen atoms, thus confirming substitution exclusively at the five-membered ring.

To elucidate whether the adjacencies of Lewis acidic metal atoms and Lewis basic phosphanyl groups give rise to intermolecular metal···P interactions, the crystal structures of the Ti complex **9a** and of all four complexes **10** and **11** were determined by X-ray diffraction analyses. As expected, **9a** is monomeric (Figure 1), whereas the corresponding PPh_2-substituted Zr and Hf complexes form centrosymmetric dimers in the isomorphous THF disolvates $(\mathbf{10a})_2$ and $(\mathbf{11a})_2$ (Figure 2) and also in the THF monosolvate of $(\mathbf{10a})_2$. In all cases, the sandwich units are linked by two

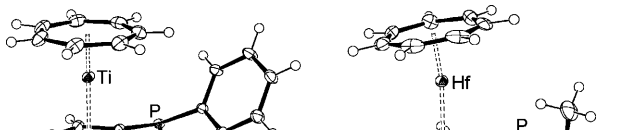

Figure 1. ORTEP diagrams of the monomeric Cht–Cp phosphane complexes **9a** (left) and **11b** (right) with thermal-displacement parameters drawn at 50% probability. Selected bond lengths [Å] and angles [°] in **9a**: Ti–C_{Cht} 2.196(1)–2.215(1), Ti–C_{Cp} 2.322(1)–2.339(1), Ti–Ct7 1.480, Ti–Ct5 1.994; Ct5-Ti-Ct7 176.6. **11b** (molecule 1/molecule 2): Hf–C_{Cht} 2.287(5)–2.313(5)/2.274(6)–2.288(6), Hf–C_{Cp} 2.439(5)–2.482(4)/2.446(4)–2.486(4), Hf–Ct7 1.614/1.618, Hf–Ct5 2.153/2.152; Ct5-Hf-Ct7 171.6/169.4.

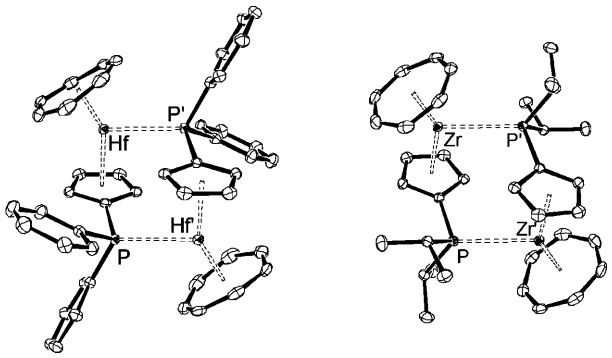

Figure 2. ORTEP diagrams of the dimeric Cht–Cp–phosphane complexes in $(\mathbf{11a})_2{\cdot}2$THF (left) and $(\mathbf{10b})_2$ (right) with thermal-displacement parameters drawn at 50% probability. Hydrogen atoms have been omitted for clarity. Selected bond lengths [Å] and angles [°] are given in Table 1.

comparatively long intermolecular metal–P bonds (Zr–P = 2.9305(4) Å in $(\mathbf{10a})_2{\cdot}$THF; Zr–P = 2.8475(3) Å in $(\mathbf{10a})_2{\cdot}2$THF, Hf–P = 2.8034(6) Å in $(\mathbf{11a})_2{\cdot}2$THF).[14,15] The pronounced difference of the Zr–P bond lengths in the mono- and disolvates of **10a** indicates a weak interaction easily influenced by external factors, such as packing. The dimeric structures can be described as adopting chair conformations, with the centroids of the Cp rings and the metal and P atoms forming the corners of six-membered rings. The relevant angles are summarized in Table 1. Similar structural motifs have been observed for other homo-dinuclear metal complexes in the absence of metal–metal bonds, for example, $[\{(\mu\text{-}\eta^5\text{-}C_5H_4PR_2)Rh(CO)\}_2]$ (R = Ph, Me),[16]

Table 1. Selected bond lengths [Å] and angles [°] in phosphane-functionalized Cht–Cp complexes.[a,b]

	(**10a**)$_2$·THF (M=Zr, R=Ph)	(**10a**)$_2$·2THF (M=Zr, R=Ph)	(**10b**)$_2$ (M=Zr, R=*i*Pr)	(**11a**)$_2$·2THF (M=Hf, R=Ph)
M–P	2.9305(4)	2.8475(3)	2.9833(3)	2.8034(6)
M–C_{Cht}	2.3489(14)–2.4547(14)	2.3395(13)–2.4545(13)	2.340(1)–2.462(1)	2.321(2)–2.450(2)
M–C_{Cp}	2.5212(13)–2.5532(13)	2.5227(12)–2.5547(12)	2.536(1)–2.562(1)	2.501(2)–2.538(2)
M–Ct7	1.750	1.746	1.761	1.726
M–Ct5	2.236	2.233	2.246	2.210
Ct5-M-Ct7	145.2	145.9	144.0	145.9
P-M-Ct5	100.7	99.1	99.9	99.1
M-Ct5-P	95.6	97.7	97.9	98.0
Ct5-P-M	108.9	110.9	107.6	110.9
P-M-Ct7	114.1	115.0	116.2	115.0

[a] Ct7 = centroid of the Cht ring. [b] Ct5 = centroid of the Cp ring.

[{(μ-η^5-$C_5H_4PPh_2$)W(CO)$_2$H}$_2$],[17] [{(μ-η^5-$C_5H_4PPh_2$)NiX}$_2$] (X = Br, CH_3),[18] [{(μ-η^5-$C_5H_4PPh_2$)PtPh}$_2$], [{(μ-η^5-$C_5H_4PPh_2$)PdMe}$_2$],[19] and [{(μ-η^5-$C_5H_4PPh_2$)Ag(PR_3)}$_2$] (R = Ph, Et).[20] Phosphane coordination leads to a marked deviation from the coplanar orientation of the Cp and Cht rings that is observed for **2** and **3**;[5] the angles subtended at the metal center by the ring centroids are 145.2/145.9° (**10a**) and 145.9° (**11a**). In all cases, the metal–carbon bonds to the seven-membered ring are significantly shorter than those to the five-membered ring, thus revealing, as expected, a significantly stronger interaction between the metal center and the cycloheptatrienyl ring.[5]

The crystal structures of the complexes bearing the sterically more demanding P*i*Pr$_2$ substituent reveal an inconsistent picture because only the Zr complex (**10b**)$_2$ is dimeric in the solid state, albeit with a Zr–P bond length of 2.9833(3) Å, which is among the longest ever observed (Figure 2).[14] In contrast, **11b** is monomeric with the shortest intra- and intermolecular Hf···P distances of 3.783 and 5.680 Å, thus excluding any metal–phosphane interaction (Figure 1). We assume that the shortening of the metal–carbon distances upon going from Zr to Hf, which is in agreement with the trend of the metal radii,[21] together with the steric bulk of the *i*Pr groups, can be considered to be responsible for preventing the dimerization of **11b**.

As described above, only one set of NMR resonance signals was observed for complexes **10** and **11** at room temperature, thus indicating fast interconversion between monomeric and dimeric species on the NMR timescale. Coalescence could be observed for **10b** by a variable-temperature ^{1}H and ^{31}P NMR study, and below approximately 173 K, two broad phosphorus resonances are generated, which can tentatively be assigned to monomeric **10b** and dimeric (**10b**)$_2$. It should be noted, however, that ambiguous broad signals additionally appear at lower field between $\delta = 4$ and 8 ppm, which again disappear upon warming to room temperature.[44] The fast equilibrium between **10b** and (**10b**)$_2$, even at low temperature, suggests the presence of only weak metal–phosphorus interactions, which is in agreement with the previously reported formation of thermodynamically labile PMe_3 adducts of trozircene (**2**)[10] and trohafcene (**3**).[5]

To theoretically assess the strength of the metal–phosphane interaction, we carried out a series of DFT calculations employing the M05–2X functional developed by Zhao and Truhlar for optimal consideration of weak noncovalent interactions.[22,23] The structures of the four monomeric complexes **10** and **11** and of the corresponding dimers were freely optimized with no geometric constraints. The resulting calculated geometries of (**10a**)$_2$, (**10b**)$_2$, and (**11a**)$_2$ are in good agreement with those established by X-ray diffraction studies (see Table 1 and the Supporting Information for coordinates and presentations of all the calculated structures).[44] For instance, the calculated P–metal distances are 2.902/2.902, 3.018/3.017, 2.869/2.869, and 3.008/2.903 Å in (**10a**)$_2$, (**10b**)$_2$, (**11a**)$_2$, and (**11b**)$_2$, respectively. The thermodynamic data for the dimerization of complexes **10** and **11** are assembled in Table 2. The formation of all the dimers is calculated to be exothermic, with ΔE values for the crystallographically observed systems (**10a**)$_2$, (**10b**)$_2$, and (**11a**)$_2$ ranging from −20.6 to −23.1 kcal mol^{-1}. The association energy for the structurally characterized monomer **11b** is found to be significantly higher ($\Delta E = -14.9$ kcal mol^{-1}), and the corresponding Gibbs free energy of $\Delta G_{298} = +10.0$ kcal mol^{-1} is in line with the inability to form the dimer (**11b**)$_2$ upon crystallization.

Table 2. Relative energies for the dimerization of complexes **10** and **11**.[a]

Dimer	ΔE [kcal mol^{-1}]	ΔH_{298} [kcal mol^{-1}]	ΔG_{298} [kcal mol^{-1}]
(**10a**)$_2$ (M = Zr, R = Ph)	−20.6	−17.9	3.0
(**10b**)$_2$ (M = Zr, R = *i*Pr)	−23.1	−19.6	−0.7
(**11a**)$_2$ (M = Hf, R = Ph)	−21.0	−18.3	0.9
(**11b**)$_2$ (M = Hf, R = *i*Pr)	−14.9	−11.1	10.0

[a] ΔE = zero-point uncorrected M05–2X electronic energies, ΔH_{298} = enthalpies at 298 K, ΔG_{298} = Gibbs free energies at 298 K.[44]

To test whether the different reactivity of the metal atoms in the P-functionalized Cht–Cp complexes **10** and **11** would have an impact on their coordination chemistry, the Ti and Zr complexes **9b** and **10b** were added to solutions of [(cod)RhCl]$_2$ (cod = η^4-1,5-cyclooctadiene) to afford the bimetallic complexes **12** and **13** (Scheme 3). The NMR spectra of both complexes are very similar, whereas the solid-state

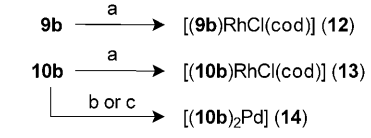

Scheme 3. Synthesis of heterobimetallic Cht–Cp phosphane complexes: a) [{(cod)RhCl}$_2$] (0.5 equiv); b) [(cod)PdCl$_2$] (0.5 equiv); c) [(η^5-C_5H_5)Pd(η^3-C_3H_5)] (0.5 equiv).

structures reveal different behavior for the Group 4 metal atoms. As expected, the troticene moiety in **12** remains unaffected by phosphane coordination, and the parallel orientation of the Cht and Cp rings is preserved (Figure 3). No

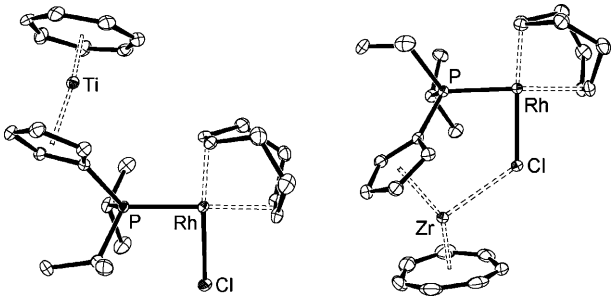

Figure 3. ORTEP diagrams of the heterobimetallic complexes **12** (left) and **13** (right) with thermal-displacement parameters drawn at 50% probability. Hydrogen atoms have been omitted for clarity. Selected bond lengths [Å] and angles [°] in **12**: Ti–C_{Cht} 2.217(3)–2.234(3), Ti–C_{Cp} 2.314(3)–2.376(3), Ti–Ct7 1.511, Ti–Ct5 2.004, Rh–P 2.3380(8), Rh–Cl 2.3713(7); Ct5-Ti-Ct7 171.4, P-Rh-Cl 90.11(3). **13**: Zr–Cl 2.7976(4), Zr–C_{Cht} 2.430(2)–2.336(2), Zr–C_{Cp} 2.521(1)–2.569(1), Zr–Ct7 1.737, Zr–Ct5 2.239, Rh–P 2.3016(4), Rh–Cl 2.3696(4); Ct5-Zr-Ct7 148.2, P-Rh-Cl 87.59(1).

additional contacts to the Ti atom are observed: the shortest Ti···Cl distance is 5.252 Å. In contrast, **13** features an intramolecular Zr–Cl contact of 2.7976(4) Å, which leads to a pronounced deviation from a coplanar Cht–Cp sandwich structure.[24] The Zr–Cl distance is very long and closely corresponds to the sum of the covalent radii that have been deduced for Zr (1.75 Å) and Cl (1.02 Å) from crystallographic data.[25] To the best of our knowledge, [ClZr(C_5H_4-PPh_2)$_2$(μ-Cl)Rh(CO)Cl] represents the only other complex containing a Zr-Cl-Rh linkage and exhibits a significantly shorter distance of 2.556(3) Å between the Zr center and the bridging Cl atom.[26]

In a similar fashion, the reaction of **10b** with [(cod)$PdCl_2$] was expected to result in the formation of [(**10b**)$_2$$PdCl_2$], which could have displayed Zr-Cl-Pd linkages.[27] However, the Pd^0 complex [(**10b**)$_2$Pd] (**14**) was instead isolated in moderate yield. Alternatively, treatment of [(η^5-C_5H_5)Pd(η^3-C_3H_5)] with two equivalents of **10b** afforded **14** as a purple–brown crystalline solid in pure form. The ^{31}P NMR spectrum shows one resonance at $\delta = 30.7$ ppm in agreement with the presence of two equivalent phosphane ligands at room temperature on the NMR timescale. In contrast, the solid-state structure of **14** reveals a T-shaped Pd complex with a Pd–Zr bond of 2.9709(3) Å (Figure 4). This bond is significantly longer than previously observed in the alkylideneamido-bridged heterobimetallic Zr/Pd complexes [Cp_2Zr(μ-N=CAr_2)$_2$PdCl(Me)] (Ar = Ph, Pd–Zr = 2.8235(5) Å; Ar = C_6H_4Me-4, Pd–Zr = 2.8416(4) Å).[28] The angles at the Pd center are P1-Pd-P2 = 131.83(2)°, P1-Pd-Zr1 = 73.65(1), and P2-Pd-Zr1 = 152.94(1)°, thus indicating a major deviation from the linear arrangement normally observed for dicoordinate structures of the type [Pd^0(PR_3)$_2$], for example, P-Pd-P = 180° in [Pd(FcP*t*Bu_2)$_2$], in which the di-*tert*-butylferrocenylphosphane (FcP*t*Bu_2) ligand is incapable of promoting a secondary Fe···Pd interaction.[29]

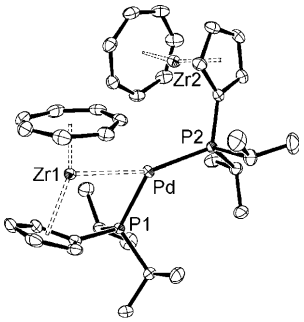

Figure 4. ORTEP diagram of the Zr_2/Pd complex **14** with thermal-displacement parameters drawn at 50% probability. Hydrogen atoms have been omitted for clarity. Selected bond lengths [Å] and angles [°]: Zr1–Pd 2.9709(3), Zr1–C_{Cht} 2.352(2)–2.420(2), Zr1–C_{Cp} 2.438(2)–2.551(2), Zr2–C_{Cht} 2.322(2)–2.364(2), Zr2–C_{Cp} 2.491(2)–2.523(2), Zr1–Ct7 1.725, Zr2–Ct7 1.669, Zr1–Ct5 2.190, Zr2–Ct5 2.201 Pd–P1 2.2417(4), Pd–P2 2.3442(4); Ct5-Zr1-Ct7 156.9, Ct5-Zr2-Ct7 166.9, P1-Pd-P2 131.83(2), Zr1-Pd-P1 73.65(1), Zr1-Pd-P2 152.94(1).

In view of the picture that has been developed for the bonding and oxidation state assignment in Cht–Cp Group 4 metal complexes,[4,5,30] the metal–metal interaction in **14** can be formally regarded as a dative $Pd^0 \rightarrow Zr^{+IV}$ bond, in which the Pd center acts as a Lewis base towards the Lewis acidic Cht–Cp sandwich moiety. This interaction is expected to be weaker than the metal–metal bonds in common "early-late" heterodimetallic complexes,[31,32] which are normally derived from the combination of an anionic late-transition metallate species with a cationic early-transition-metal complex fragment. To estimate the strength of the Pd–Zr bond in **14**, we performed theoretical calculations on the bridged model complex [{(η^7-C_7H_7)Zr(η^5-$C_5H_4PMe_2$)}Pd(PMe_3)] (**15**) and [{(η^7-C_7H_7)Zr(η^5-C_5H_5)}Pd(PMe_3)$_2$] (**16**), in which trozircene (**2**) interacts with [Pd(PMe_3)$_2$] in an intermolecular fashion. Again, the M05–2X functional was employed,[22] which has also performed well for predicting the energetics of van der Waals metal dimers.[33] For both complexes, the optimized molecular structures feature a Pd···Zr interaction with Pd–Zr = 3.320 and 3.156 Å for **15** and **16**, respectively (Figure 5).

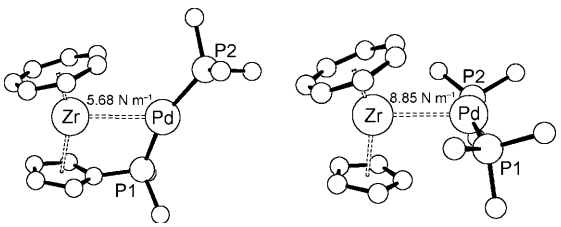

Figure 5. PLUTO drawings of the optimized molecular structures of **15** and **16** at the M05–2X level of theory and relaxed Pd–Zr force constants. Selected bond lengths [Å] and angles [°] in **15**/**16**: Zr–Pd 3.320/3.156, Pd–P1 2.271/2.336, Pd–P2 2.382/2.336; Ct5-Zr-Ct7 156.3/154.0, P-Pd-P 160.9/158.3.[44]

Because geometrical parameters are not ideal bond-strength descriptors, in particular in the case of weak interactions,[34] we additionally computed relaxed force constants.[35] The results indeed point to a very weak noncovalent Pd···Zr interaction, which is reflected by the very small values of 5.68 and 8.85 $N\,m^{-1}$ for **15** and **16** (or 0.0568 and 0.0885 $mdyn\,Å^{-1}$, respectively).[36] This finding means that a shortening of the Pd···Zr distance in **15** by 0.35 Å to comply with the experimentally derived value of approximately 2.97 Å (Figure 4) affords an energy penalty of only 0.5 $kcal\,mol^{-1}$,[37] in line with an extremely flat potential-energy surface. Naturally, the Pd···Zr bond-dissociation energy could only be calculated for the unbridged model complex **16**, thus resulting in $\Delta E_{diss} = 10.5\ kcal\,mol^{-1}$. This value, albeit small, falls in the same range that has been derived for trozircene–isocyanide adducts,[9] thus indicating that complexes such as **16** that feature unsupported Pd–Zr bonds should also be isolable.[38]

Conclusion

Upon complexation, the presence of Lewis acidic Cht-Cp metal moieties in the zirconium–phosphane and hafnium–phosphane ligands **10** and **11** gives rise to unusual secondary interactions involving the formation of weak dative bonds. Thereby, the Zr and Hf atoms act as acceptor sites in a similar fashion to that described for ambiphilic phosphane ligands featuring pendant borane and alane moieties, which have also been investigated as promising candidates for organotransition metal catalysis, notably through intramolecular activation of the M–X bonds.[39] Similarly, the bifunctional reactivity of **10** and **11** should have an impact on the activation of substrates, for example, by oxidative addition to complexes such as **14**, and the exploration of their potential for applications in homogeneous catalysis will be the subject of future studies.

Experimental Section

General: All operations were performed in a glovebox in a dry argon atmosphere (MBraun 200B) or on a high-vacuum line using Schlenk techniques. All solvents were purified by a solvent-purification system from MBraun GmbH and stored over molecular sieves (4 Å) prior to use. The ^{1}H, ^{13}C, and ^{31}P NMR spectra were recorded on Bruker DPX 200 (200 MHz), Bruker AV 300 (300 MHz), and Bruker DRX 400 (400 MHz) devices. The chemical shifts are expressed in parts per million (ppm) with tetramethylsilane (TMS) as an internal standard. Coupling constants (J) are reported in Hertz (Hz), and splitting patterns are indicated as s (singlet), d (doublet), t (triplet), q (quartet), vq (virtual quartet), m (multiplet), sept (septet), and br (broad). Elemental analysis (C, H, N) succeeded by combustion and gas chromatographic analysis with an Elementar varioMICRO and HRMS from Bruker-Demo QTOF micro. The starting materials were obtained either from Aldrich or Alfa Aesar and were used without further purification. The following compounds were synthesized according to reported methods: $[(\eta^5\text{-}C_5H_4PPh_2)TiCl_3]$ (**6a**),[13] $[(C_5H_4PPh_2)Li]$,[12] $[(C_5H_4PiPr_2)Li]$,[12] $[(\eta^5\text{-}C_5H_4PPh_2)_2ZrCl_2]$ (**7a**),[12] $[(\eta^5\text{-}C_5H_4PiPr_2)_2ZrCl_2]$ (**7b**),[12] $[(\eta^5\text{-}C_5H_5)Pd(\eta^3\text{-}C_3H_5)]$,[40] and $[\{(cod)RhCl\}_2]$.[41]

$[(\eta^5\text{-}C_5H_4PiPr_2)TiCl_3]$ (6b): $C_5H_4(SiMe_3)PiPr_2$ was prepared in an analogous manner to that described for $C_5H_4(SiMe_3)PPh_2$.[13] This cyclopentadiene (1.69 g, 6.54 mmol) in toluene (20 mL) was added dropwise to $[TiCl_4]$ (1.24 g, 6.54 mmol) in toluene (20 mL) at ambient temperature. An immediate color change was observed, and the purple solution was stirred for 1 h at room temperature. After evaporation of all volatiles, the product was isolated as a deep-red oil in 81% yield (1.77 g, 5.30 mmol). ^{1}H NMR (200 MHz, $CDCl_3$): $\delta = 6.71$ (m, 4H; C_5H_4), 1.78 (sept, 2H; CH), 1.15 (dd, $^{3}J_{HP} = 7.07$ Hz, 6H; CH_3), 1.03 ppm (dd, $^{3}J_{HP} = 7.05$ Hz, 6H; CH_3); $^{13}C\{^{1}H\}$ NMR (53 MHz, $CDCl_3$): $\delta = 130.5$ (d, $^{1}J_{CP} = 17.06$ Hz, *i*-C_5H_4), 125.8 (d, $^{2}J_{CP} = 7.46$ Hz, α-C_5H_4), 125.1 (br s, β-C_5H_4), 24.2 (d, $^{1}J_{CP} = 14.78$ Hz, CH), 20.2 (d, $^{2}J_{CP} = 12.17$ Hz, CH_3), 19.9 ppm (d, $^{2}J_{CP} = 14.09$ Hz, CH_3); $^{31}P\{^{1}H\}$ NMR (82 MHz, $CDCl_3$): $\delta = 14.47$ (s, PCH-$(CH_3)_2$); MS (EI): m/z (%): 339 $[M]^+$, 299 $[M^+-Cl]$, 182 $[299-P(CH(CH_3)_2)_2]$, 182 $[C_5H_4P(CH(CH_3)_2)_2]$, 147 $[182-Cl]$, 139 $[182-CH(CH_3)_2]$; elemental analysis (%) calcd for $C_{11}H_{18}Cl_3TiP$ (335.5): C 39.38, H 5.41; found: C 39.72, H 5.75.

$[(\eta^5\text{-}C_5H_4PPh_2)_2HfCl_2]$ (8a): $[HfCl_4]$ (1.00 g, 3.12 mmol) was treated with $[(C_5H_4PPh_2)Li]$ (2 equiv) in toluene (60 mL) and THF (2 mL) at −78 °C. The reaction mixture was allowed to warm to room temperature overnight and was subsequently heated at 80 °C for an additional hour. The solution was filtered through a plug of celite, and the filtrate was concentrated to about 5 mL. The off-white product was precipitated by addition of pentane (60 mL), isolated by filtration, dried in vacuo, and obtained in a 65% yield (1.51 g, 2.11 mmol). ^{1}H NMR (300 MHz, CD_2Cl_2): $\delta = 7.24$ (m, 20H; C_5H_6), 6.17 ppm (m, 8H; C_5H_4); $^{13}C\{^{1}H\}$ NMR (75 MHz, CD_2Cl_2): $\delta = 137.6$ (d, $^{1}J_{CP} = 12.2$ Hz, *i*-C_6H_5), 134.3 (d, $^{2}J_{CP} = 20.77$ Hz, *o*-C_6H_5), 129.6 (s, *p*-C_6H_5), 128.9 (d, $^{3}J_{CP} = 7.37$ Hz, *m*-C_6H_5), 123.3 (d, $^{1}J_{CP} = 16.33$ Hz, *i*-C_5H_4), 121.8 (d, $^{2}J_{CP} = 9.98$ Hz, α-C_5H_4), 116.9 ppm (s, β-C_5H_4); $^{31}P\{^{1}H\}$ NMR (121 MHz, CD_2Cl_2): $\delta = -17.3$ ppm (s, PPh_2); elemental analysis (%) calcd for $C_{34}H_{28}Cl_2P_2Hf$ (747.9): C 54.60, H 3.77; found: C 54.77, H 3.97.

$[(\eta^5\text{-}C_5H_4PiPr_2)_2HfCl_2]$ (8b): $[HfCl_4]$ (796.3 mg, (2.49 mmol) was treated with $[(C_5H_4PiPr_2)Li]$ (2 equiv) in toluene (60 mL) and THF (0.5 mL) at −78 °C. The reaction mixture was allowed to warm to room temperature overnight and was subsequently heated at 70 °C for an additional hour. The solution was filtered through a plug of celite, and the filtrate was concentrated to about 3 mL. The off-white product was precipitated by the addition of pentane (60 mL), isolated by filtration, dried in vacuo, and obtained in 69% yield (1.045 g, 1.708 mmol). ^{1}H NMR (300 MHz, CD_2Cl_2): $\delta = 6.55$ (m, 4H; α-C_5H_4), 6.36 (m, 4H; β-C_5H_4), 1.96 (sept d, $^{2}J_{HP} = 1.72$ Hz, 4H; CH), 1.09 (dd, $^{3}J_{HP} = 13.8$, $^{3}J_{HH} = 7.1$ Hz, 6H; CH_3), 0.91 ppm (dd, $^{3}J_{HP} = 12.7$, $^{3}J_{HH} = 7.0$ Hz, 6H; CH_3); $^{13}C\{^{1}H\}$ NMR (75.47 MHz, CD_2Cl_2): $\delta = 122.6$ (m α-C_5H_4), 122.3 (d, $^{1}J_{CP} = 29.37$ Hz, *i*-C_5H_4), 116.8 (m, β-C_5H_4), 24.1 (d, $^{1}J_{CP} = 12.79$ Hz, CH), 20.4 (d, $^{2}J_{CP} = 13.15$ Hz, CH_3), 20.2 ppm (d, $^{2}J_{CP} = 13.55$ Hz, CH_3); $^{31}P\{^{1}H\}$ NMR (121.49 MHz, CD_2Cl_2): $\delta = 5.2$ ppm (s, $P(CHCH_3)_2$); elemental analysis (%) calcd for $C_{22}H_{36}Cl_2P_2Hf$ (611.9): C 43.19, H 5.93; found: C 43.59, H 5.97.

$[(\eta^7\text{-}C_7H_7)Ti(\eta^5\text{-}C_5H_4PPh_2)]$ (9a): Magnesium turnings (0.66 g, 27.26 mmol), anhydrous ferric chloride (catalytic amount), and cycloheptatriene (1.42 mL, 13.69 mmol) were suspended in THF (20 mL). A solution of **6a** (3.15 g, 7.79 mmol) THF (20 mL) was added dropwise. The reaction mixture was stirred for 12 h at room temperature followed by evaporation of the solvent. The residue was suspended in toluene (50 mL) and filtered. After evaporation of the solvent, the residue was dissolved in hexane followed by an additional filtration. After removal of the solvent, **9a** was isolated as a green solid in 75% yield (2.27 g, 5.84 mmol). Crystals suitable for X-ray diffraction studies could be obtained by cooling a saturated solution of **9a** in hexane. ^{1}H NMR (200 MHz, C_6D_6): $\delta = 7.37$ (m, 4H; *o*-C_6H_5), 7.04 (m, 6H; C_6H_5), 5.42 (s, 7H; C_7H_7), 5.05 ppm (m, 4H; C_5H_4); $^{13}C\{^{1}H\}$ NMR (53 MHz, C_6D_6): $\delta = 140.7$ (s, *i*-C_6H_5), 136.2 (s, *o*-C_6H_5), 135.8 (s, *p*-C_6H_5), 135.6 (s, *m*-C_6H_5), 109.3 (s, *i*-C_5H_4), 103.3 (s, α-C_5H_4), 100.3 (s, β-C_5H_4), 87.9 ppm (s, C_7H_7); $^{31}P\{^{1}H\}$ NMR (82 MHz, C_6D_6): $\delta = -17.45$ (s, $P(C_6H_5)_2$); elemental analysis (%) calcd for $C_{24}H_{21}PTi$ (388.3): C 74.24, H 5.45; found: C 74.44, H 5.50.

[(η⁷-C_7H_7)Ti(η⁵-$C_5H_4PiPr_2$)] (9b): Magnesium turnings (0.39 g, 16.14 mmol), anhydrous ferric chloride (catalytic amount), and cycloheptatriene (0.84 mL, 8.11 mmol) were suspended in THF (10 mL). A solution of **6b** (1.54 g, 4.61 mmol) in THF (25 mL) was added dropwise at ambient temperature. After stirring for 12 h at room temperature, the solvent was removed in vacuo, the residue was dissolved in toluene (40 mL), and the solution was filtered. After evaporation of the solvent, the residue was dissolved in hexane and filtered again. Removal of the solvents afforded **9b** as a green oil in 74% yield (1.09 g, 3.14 mmol). ^{1}H NMR (200 MHz, C_6D_6): δ = 5.37 (s, 7H; C_7H_7), 4.93 (m, 4H; C_5H_4), 1.59 (sept, 2H; C*H*(CH_3)$_2$), 0.88 (dd, $^3J_{HP}$ = 13.02, $^3J_{HH}$ = 7.07 Hz, 6H; CH(C*H*$_3$)$_2$), 0.80 ppm (dd, $^3J_{HP}$ = 12.31, $^3J_{HH}$ = 7.05 Hz, 6H; CH(C*H*$_3$)$_2$); ^{13}C{^{1}H} NMR (50 MHz, C_6D_6): δ = 106.3 (d, $^1J_{CP}$ = 8.58 Hz, *i*-C_5H_4), 100.9 (d, $^2J_{CP}$ = 10.08 Hz, α-C_5H_4), 98.8 (d, $^3J_{CP}$ = 2.45 Hz, β-C_5H_4), 87.4 (s, C_7H_7), 24.4 (d, $^1J_{CP}$ = 13.93 Hz, CH), 20.4 (d, $^2J_{CP}$ = 5.98 Hz, CH_3), 20.2 ppm (d, $^2J_{CP}$ = 8.39 Hz, CH_3); ^{31}P{^{1}H} NMR (C_6D_6, 82 MHz): δ = 3.31 ppm (s, P($CHCH_3$)$_2$); MS (EI): *m*/*z* (%): 320 ([*M*]$^+$, 25), 204 ([*M*$^+$ −P(CH((CH_3)$_2$)$_2$)], 5), 139 ([*M*$^+$−CpP{CH[(CH_3)$_2$]$_2$}], 25), 91 ([C_7H_7], 70+).

[(η⁷-C_7H_7)Zr(η⁵-$C_5H_4PPh_2$)] (10a): A solution of **7a** (1.23 g, 1.70 mmol) dissolved in THF (20 mL) was added to a mixture of magnesium turnings (0.146 g, 5.951 mmol), anhydrous ferric chloride (catalytic amount), and cycloheptatriene (0.35 mL, 3.40 mmol) in THF (30 mL). The reaction mixture was stirred overnight, filtered, and evaporated to dryness. Compound **10a** was sublimed at 160 °C/10^{-3} mbar to afford an orange solid. Orange crystals suitable for X-ray diffraction studies were grown by diffusion of hexane into a saturated solution of **10a** in THF to obtain a 23% yield (168 mg, 0.72 mmol). ^{1}H NMR (300 MHz, [D_8]THF): δ = 7.45 (m, 4H; *o*-C_6H_5), 7.30 (m, 6H; C_6H_5), 5.73 (br t, 2H; α-C_5H_4), 5.16 (m, 2H; β-C_5H_4), 4.63 ppm (s, C_7H_7); ^{13}C{^{1}H} NMR (75 MHz, [D_8]THF): δ = 140.6 (d, $^1J_{CP}$ = 11.28 Hz, *i*-C_6H_5), 133.8 (d, $^2J_{CP}$ = 19.59 Hz, *o*-C_6H_5), 128.5 (s, *p*-C_6H_5), 128.6 (d, $^3J_{CP}$ = 6.74 Hz, *m*-C_6H_5), 107.9 (brs, *i*-C_5H_4), 106.8 (d, $^2J_{CP}$ = 15.65 Hz, α-C_5H_4), 101.6 (d, $^3J_{CP}$ = 4.69 Hz, β-C_5H_4), 80.8 ppm (s, C_7H_7); ^{31}P{^{1}H} NMR: (121 MHz, [D_8]THF): −21.5 ppm (s, PPh_2), HR-MS (EI): *m*/*z*: calcd for monoisotopic mass for [$C_{24}H_{21}PZr$]$^+$: 430.0428; found: 430.0422.

[(η⁷-C_7H_7)Zr(η⁵-$C_5H_4PiPr_2$)] (10b): A mixture of magnesium turnings (132.6 mg, 5.454 mmol), freshly distilled cycloheptatriene (0.26 mL, 0.335 mg, 3.636 mmol), and cat. $FeCl_3$ (2.3 mg, 0.014 mmol) was stirred in THF (20 mL) at room temperature followed by the addition of **7a** (661.1 mg, 1.818 mmol) dissolved in THF (30 mL). The yellow solution was stirred overnight and a color change from yellow to deep purple and further to black–brown could be observed. The reaction mixture was filtered, the solvent evaporated in vacuo, and the dark-brown residue was sublimed at 150 °C/5×10^{-3} mbar to obtain **10b** as a deep purple solid in a moderate yield of 22% (98.9 mg, 0.272 mmol). Crystals for X-ray structure determination were obtained by slow evaporation of the solvent from a saturated solution of **10b** in hexane. ^{1}H NMR (400 MHz, C_6D_6): δ = 5.49 (br, 2H; α-C_5H_4), 5.42 (m, 2H; β-C_5H_4), 5.26 (s, 7H; C_7H_7), 1.68 (sept d, $^2J_{HP}$ = 0.88 Hz, 2H; CH), 0.98 (dd, $^3J_{HP}$ = 14.29, $^3J_{HH}$ = 6.95 Hz, 6H; CH_3), 0.87 ppm (dd, $^3J_{HP}$ = 11.33, $^3J_{HH}$ = 7.08 Hz, 6H; CH_3); ^{13}C{^{1}H} NMR (100 Hz, C_6D_6) δ 111.9 (d, $^1J_{CP}$ = 24.88 Hz, *i*-C_5H_4), 105.6 (d, $^2J_{CP}$ = 11.27 Hz, α-C_5H_4), 103.1 (dd, $^3J_{CP}$ = 2.97 Hz, β-C_5H_4), 81.3 (s, C_7H_7), 23.9 (d, $^1J_{CP}$ = 13.55 Hz, CH), 20.2 (d, $^2J_{CP}$ = 6.61 Hz, CH_3), 20.0 ppm (br, CH_3); ^{31}P{^{1}H} NMR (161 MHz, C_6D_6): δ = 0.00 ppm (s, P[CH(CH_3)$_2$]); elemental analysis (%) calcd for $C_{18}H_{25}PZr$ (363.6): C 59.46, H 6.93; found: C 59.27, H 7.01.

[(η⁷-C_7H_7)Hf(η⁵-$C_5H_4PPh_2$)] (11a): Compound **8a** (1.159 g, 1.55 mmol) dissolved in THF (10 mL) was added to a suspension magnesium turnings (0.113 g, 4.65 mmol, 3 equiv), cycloheptatriene (0.32 mL, 3.10 mmol, 2 equiv), and $FeCl_3$ (2.3 mg) in THF (20 mL). The reaction mixture was stirred for 3 days at 65 °C and the solution turned brown. After filtration the solvent was removed in vacuo. The black–brown residue was sublimed at 175 °C/5×10^{-3} mbar to obtain **11a** as an orange–red solid in 14% yield (90.3 mg, 0.174 mmol). Single crystals suitable for X-ray diffraction studies were obtained by diffusion of hexane into a saturated solution of **11a** in THF at room temperature. ^{1}H NMR (300 MHz, THF-d_8): δ = 7.28 (m, 10H; C_6H_5), 5.76 (m, 2H; α-C_5H_4), 5.34 (m, 2H; β-C_5H_4), 4.77 ppm (s, 7H; C_7H_7); ^{13}C{^{1}H} NMR (75 MHz, [D_8]THF): δ = 139.9 (d, $^1J_{CP}$ = 11.04 Hz, *i*-C_6H_5), 133.7 (d, $^2J_{CP}$ = 19.88 Hz, *o*-C_6H_5), 128.8 (s, *p*-C_6H_5), 128.4 (d, $^3J_{CP}$ = 7.00 Hz, *m*-C_6H_5), 109.3 (s, *i*-C_5H_4), 104.8 (d, $^2J_{CP}$ = 14.89 Hz, α-C_5H_4), 101.1 (d, $^3J_{CP}$ = 4.45 Hz, β-C_5H_4), 77.2 ppm (s, C_7H_7); ^{31}P{^{1}H} NMR: (121 MHz, [D_8]THF): −21.7 (s, PPh_2); elemental analysis (%) calcd for $C_{24}H_{21}PHfC_4H_8O$ (591.0): C 56.90, H 4.95; found: C 57.24, H 4.50.

[(η⁷-C_7H_7)Hf(η⁵-$C_5H_4PiPr_2$)] (11b): Compound **8b** (1.21 mg, 2.00 mmol) dissolved in THF (10 mL) was added to a suspension of magnesium turnings (114 mg, 5.99 mmol), cycloheptatriene (0.20 mL, 3.99 mmol), and $FeCl_3$ (5.2 mg) in THF (10 mL). The reaction mixture was stirred for 5 days at 65 °C. The solvent was evaporated, toluene (20 mL) was added, and the orange–brown solution was filtered. After evaporation of the solvent, the brown residue was sublimed at 175 °C/3×10^{-3} mbar. Compound **11b** was obtained as orange–red solid in 21% yield (184.3 mg, 0.41 mmol). Single crystals were grown by cooling a saturated solution of **11b** in toluene to −35 °C. ^{1}H NMR (400 MHz, C_6D_6): δ = 5.37 (br, 2H; α-C_5H_4), 5.36 (br, 2H; β-C_5H_4), 5.14 (s, 7H; C_7H_7), 1.69 (sept d, $^2J_{HP}$ = 1.16 Hz, 2H; CH), 0.98 (dd, $^3J_{HP}$ = 14.13, $^3J_{HH}$ = 7.18 Hz, 6H; CH_3), 0.88 ppm (dd, $^3J_{HP}$ = 11.81, $^3J_{HH}$ = 7.00 Hz, 6H; CH_3); ^{13}C{^{1}H} NMR (100 Hz, C_6D_6): δ = 110.8 (s, *i*-C_5H_4), 103.2 (d, $^2J_{CP}$ = 11.28 Hz, α-C_5H_4), 100.47 (d, $^3J_{CP}$ = 2.43 Hz, β-C_5H_4), 77.5 (s, C_7H_7), 24.3 (d, $^1J_{CP}$ = 14.3 Hz, CH), 20.2 (d, $^2J_{CP}$ = 3.56 Hz, CH_3), 20.1 ppm (d, $^2J_{CP}$ = 9.71 Hz, CH_3); ^{31}P{^{1}H} NMR (161 MHz, C_6D_6): δ = 0.01 ppm (s, P[CH(CH_3)$_2$]); elemental analysis (%) calcd for $C_{18}H_{25}PHf$ (450.9): C 47.95, H 5.59; found: C 48.18, H 5.56.

[(9b)RhCl(cod)] (12): Compound **6b** (76.3 mg, 0.24 mmol) dissolved in hexane (5 mL) was added to bis-μ-chloro-(η⁴-1,5-cyclooctadiene)dirhodium (59.0 mg, 0.12 mmol) in toluene (3 mL). The reaction mixture was stirred for 2 h. During the reaction time, the solution darkened and a precipitate formed, which was filtered off and dried in vacuo. Compound **12** was obtained as a light-green solid in 42% yield (56.6 mg, 0.10 mmol). Suitable crystals for X-ray diffraction studies were obtained on cooling a saturated solution of **12** in THF/hexane. ^{1}H NMR (200 MHz, C_6D_6): δ = 5.63 (br, 2H; vinyl cod), 5.47 (s, 7H; C_7H_7), 5.05 (m, 2H; α-C_5H_4), 4.98 (m, 2H; β-C_5H_4), 3.28 (br, 2H; vinyl cod), 2.66 (sept, 2H; CH), 2.11 (m, 4H; allyl cod), 1.36 (m, 4H; allyl cod), 1.46 (dd, $^3J_{HP}$ = 15.02, $^3J_{HH}$ = 7.15 Hz, 6H; CH_3), 1.22 ppm (dd, $^3J_{HP}$ = 14.92, $^3J_{HH}$ = 7.15 Hz, 6H; CH_3); ^{13}C{^{1}H} NMR (100 MHz, C_6D_6): δ = 110.4 (d, $^1J_{CP}$ = 11.89 Hz, *i*-C_5H_4), 102.5 (m, cod), 101.7 (d, $^2J_{CP}$ = 6.77 Hz, α-C_5H_4), 98.4 (d, $^3J_{CP}$ = 6.39 Hz, β-C_5H_4), 87.78 (s, C_7H_7), 68.1 (d, $^1J_{CRh}$ = 14.22 Hz, cod), 33.4 (d, $^2J_{CRh}$ = 2.61 Hz, cod), 28.8 (brs, cod), 28.3 (br, cod), 28.1 (br, cod), 24.5 (br, CH), 20.6 (brs, *C*H$_3$), 20.1 ppm (d, $^2J_{CP}$ = 3.29 Hz, CH_3); ^{31}P NMR (162 MHz, C_6D_6): δ = 36.63 ppm (d, $^1J_{PRh}$ = 151.1 Hz, P[C(CH_3)$_2$]$_2$); elemental analysis (%) calcd for $C_{26}H_{37}PTiRh$ (531.3): C 55.10, H 6.58; found: C 52.55, H 6.22.

[(10b)RhCl(cod)] (13): Compound **10b** (111.3 mg, 0.31 mmol) dissolved in hexane (12 mL) was added dropwise at ambient temperature to a solution of [{(cod)RhCl}$_2$] (75.5 mg, 0.15 mmol) in toluene (3 mL). An orange solid was formed immediately and after 15 min of stirring was collected by filtration and washed with hexane (3×3 mL) to give **13** in 88% yield (165.0 mg, 0.27 mmol). Suitable single crystals for X-ray structure analyses were obtained by diffusion of hexane into a saturated solution of **13** in toluene. ^{1}H NMR (400 MHz, C_6D_6): δ = 5.56 (m, 2H; α-C_5H_4), 5.49 (m, 2H; β-C_5H_4), 5.23 (brs, 2H; vinyl H), 5.11 (s, 7H; C_7H_7), 3.41 (brs, 2H; vinyl H), 2.05 (m, 2H; CH_2), 1.93 (m, 2H; CH_2), 1.62 (m, 4H; CH_2), 1.49 (sept, $^3J_{HH}$ = 6.8 Hz, 2H; CH), 1.15 (dd, $^3J_{HP}$ = 13.5, $^3J_{HH}$ = 6.8 Hz, 6H; CH_3), 0.79 (dd, $^3J_{HP}$ = 15.2, $^3J_{HH}$ = 6.8 Hz, 6 ppm H; CH_3); ^{13}C{^{1}H} NMR (100 MHz, C_6D_6): δ = 112.2 (d, $^1J_{CP}$ = 11.18 Hz, *i*-C_5H_4), 105.3 (d, $^2J_{CP}$ = 8.75 Hz, α-C_5H_4), 103.7 (m, cod), 103.5 (m, cod), 100.8 (d, $^2J_{CP}$ = 8.24 Hz, β-C_5H_4), 81.9 (s, C_7H_7), 69.4 (d, $^1J_{CRh}$ = 13.93 Hz, cod), 33.2 (d, $^2J_{CRh}$ = 2.40 Hz, cod), 28.3 (d, $^2J_{CRh}$ = 1.20 Hz, cod), 23.5 (brs, CH), 23.3 (m, cod), 19.9 (d, $^2J_{CP}$ = 3.32 Hz, CH_3), 19.2 ppm (brs, CH_3); ^{31}P{^{1}H} NMR (161.98 MHz, C_6D_6): δ = 37.5 ppm (d, $^1J_{PRh}$ = 144.1 Hz, P[CH(CH_3)$_2$]; elemental analysis (%) calcd for $C_{26}H_{37}ClPRhZr$ (610.1): C 51.18, H 6.11; found: C 51.12, H 6.10.

[(10b)$_2$Pd] (14): Compound **10b** (294.9 mg, 0.81 mmol) and [(η⁵-C_5H_5)Pd(η³-C_3H_5)] (85.8 mg, 0.41 mmol) in toluene (20 mL) were stirred

at 75 °C overnight. The solvent was removed in vacuo, and the dark-red oily residue was dried at 40 °C in vacuo. The residue was dissolved in the minimum amount of THF and added to a rapidly stirred mixture of hexamethyldisiloxane/hexane (4:1). A purple–brown microcrystalline solid precipitated and was collected on a Schlenk sinter, washed with hexamethyldisiloxane, and dried in vacuo to give **10** in 37% yield (125.7 mg, 0.15 mmol). Crystals were obtained by cooling a solution of **14** in hexamethyldisiloxane/hexane to −35 °C. ^{1}H NMR (300 MHz, C_6D_6): $\delta = 5.66$ (m, 4H; α-C_5H_4), 5.46 (s, 14H; C_7H_7), 5.42 (m, 4H; δ-C_5H_4), 1.89 (m, 4H; CH), 1.19 (vq, $^3J_{HH} = 14.91$, $^3J_{HP} = 7.19$ Hz, 12H; CH_3), 1.09 ppm (vq, $^3J_{HH} = 16.07$, $^3J_{HP} = 6.89$ Hz, 12H; CH_3); ^{13}C{^{1}H} NMR (75 MHz, C_6D_6): 104.1 (m, *i*-C_5H_4), 103.7 (m, α-C_5H_4), 101.4 (β-C_5H_4), 79.2 (C_7H_7), 25.9 (t, CH), 20.5 (t, CH_3), 20.2 ppm (t, CH_3); ^{31}P{^{1}H} NMR (121 MHz, C_6D_6): $\delta = 30.7$ (s, P-$(CHCH_3)_2$); elemental analysis (%) calcd for $C_{36}H_{50}P_2PdZr_2$ (833.6): C 51.87, H 6.05; found: C 51.76, H 6.25.

Computational details: The computations were performed using the hybrid density functional method M05-2X, which is implemented in the Gaussian 03 program package.[42] For all main-group elements (C, H, P), the all-electron triple-ζ basis set (6-311G**) was used, whereas for all transition-metal elements (Zr, Hf, Pd) the effective core potential double-ζ basis set (Stuttgart RSC 1997 ECP) was applied.[43] The Pd–Zr bond dissociation energy ΔE_{diss} for the unbridged Zr/Pd complex [{(η^7-C_7H_7)Zr(η^5-C_5H_5)}Pd-$(PMe_3)_2$] (**16**) was calculated by subtracting the energies of the ground-state electronic structures of **2** and [Pd$(PMe_3)_2$] from that of **16**. Further details together with presentations and coordinates in *x,y,z* format of all optimized structures can be found in the Supporting Information.[44]

Single-crystal X-ray structure determinations: Data were recorded on various area detectors (Bruker, Oxford Diffraction) at low temperature. Structures were refined anisotropically using the program SHELXL-97.[45] Hydrogen atoms were included using rigid methyl groups or a riding model. Pertinent data are summarized in Table 3.

Special features: The Flack parameters for the noncentrosymmetric structures of **9a**, **12**, and **13** were refined to −0.008(14), 0.03(2), and −0.005(12), respectively. CCDC-706212, CCDC-706213, CCDC-706214, CCDC-706215, CCDC-706216, CCDC-706217, CCDC-706218, CCDC-706219, and CCDC-711402 contain the supplementary crystallographic data for this paper. These data can be obtained free of charge from The Cambridge Crystallographic Data Centre via www.ccdc.cam.ac.uk/data_request/cif

Acknowledgements

This work was supported by the Deutsche Forschungsgemeinschaft (DFG) through grant Ta 189/5-3. We thank Priz.-Doz. Jörg Grunenberg and Dipl.-Chem. Kai Brandhorst for helpful discussions.

Table 3. Crystallographic data.

	9a	**10a**·THF	**10a**·2 THF	**10b**	**11a**·2 THF	**11b**	**12**	**13**	**14**
empirical formula	$C_{24}H_{21}PTi$	$C_{52}H_{50}OP_2Zr_2$	$C_{56}H_{58}O_2P_2Zr_2$	$C_{36}H_{50}P_2Zr_2$	$C_{56}H_{58}Hf_2O_2P_2$	$C_{36}H_{50}Hf_2P_2$	$C_{26}H_{37}ClPRhTi$	$C_{26}H_{37}ClPRhZr$	$C_{36}H_{50}P_2PdZr_2$
formula weight	388.28	935.30	1007.40	727.14	1181.94	901.68	566.79	610.11	833.54
T [°C]	−173	−140	−173	−140	−140	−173	−173	−140	−140
λ [Å]	0.71073	0.71073	0.71073	0.71073	0.71073	0.71073	0.71073	0.71073	0.71073
crystal system	orthorhombic	monoclinic	monoclinic	monoclinic	monoclinic	orthorhombic	monoclinic	orthorhombic	triclinic
space group	$P2_12_12_1$	$C2/c$	$P2_1/n$	$C2/c$	$P2_1/n$	$Pbca$	$P2_1$	$P2_12_12_1$	$P\bar{1}$
a [Å]	9.5387(4)	21.4115(14)	13.4714(3)	19.3162(10)	13.5111(16)	8.1356(3)	7.7561(8)	8.0594(8)	10.9736(10)
b [Å]	11.6353(5)	19.1843(6)	12.3274(3)	10.2321(6)	12.4013(14)	22.9414(4)	15.5516(18)	13.8676(12)	12.2949(10)
c [Å]	17.0221(8)	19.1642(14)	13.5669(3)	16.2273(10)	13.5425(16)	36.6038(8)	9.8927(10)	21.887(2)	13.3191(12)
α [°]	90	90	90	90	90	90	90	90	83.521(3)
β [°]	90	96.985(3)	98.605(3)	102.178(3)	98.395(3)	90	90.035(6)	90	73.780(3)
γ [°]	90	90	90	90	90	90	90	90	80.454(3)
V [Å^3]	1889.21(14)	4148.0(5)	2227.66(9)	3135.1(3)	2244.8(5)	6831.8(3)	1193.3(2)	2446.2(4)	1697.4(3)
Z	4	4	2	4	2	8	2	4	2
crystal size [mm^3]	0.24×0.14×0.11	0.24×0.38×0.47	0.26×0.25×0.18	0.20×0.22×0.36	0.36×0.33×0.26	0.18×0.15×0.14	0.14×0.13×0.09	0.39×0.35×0.21	0.33×0.27×0.21
$2\theta_{max}$ [°]	64	61	56	61	61	61	71	60	61
reflections collected	82796	43435	67477	31107	47476	208907	31348	52933	36089
independent reflections	6748	6328	5530	4827	6851	10409	8004	7482	10271
max./min. transmission	0.9428/0.8182	0.8656/0.7595	1.00000/0.96837	0.8577/0.7636	0.3723/0.2804	1.00000/0.85661	0.8984/0.8481	0.7738/0.6337	0.7800/0.6906
goodness of fit	1.070	1.038	1.069	1.053	1.051	1.125	1.011	1.056	1.064
F(000)	808	1920	1040	1504	1168	3520	584	1240	844
ρ_{calcd} [g cm^{-3}]	1.365	1.498	1.502	1.541	1.749	1.753	1.577	1.657	1.631
μ [mm^{-1}]	0.542	0.619	0.584	0.792	4.737	6.190	1.217	1.287	1.245
$R_1(I > 2\sigma(I))$	0.0288	0.0249	0.0192	0.0176	0.0167	0.0392	0.0370	0.0140	0.0220
wR_2	0.0719	0.0675	0.0530	0.0494	0.0390	0.0664	0.0801	0.0360	0.0565
$\Delta\rho$ [e Å^{-3}]	0.504/−0.208	1.147/−1.175	0.379/−0.418	0.468/−0.389	1.298/−0.455	2.419/−4.574	1.675/−1.008	0.366/−0.414	0.654/−0.410

[1] Special Issue: 50th Anniversary of the Discovery of Ferrocene *J. Organomet. Chem.* **2001**, *637–639*, 1 edited by R. D. Adams.
[2] *Ferrocenes* (Eds.: A. Togni, T. Hayashi), VCH, Weinheim, **1995**.
[3] a) A. Fihri, P. Meunier, J.-C. Hierso, *Coord. Chem. Rev.* **2007**, *251*, 2017–2055; b) R. G. Arrayás, J. Adrio, J. C. Carretero, *Angew. Chem.* **2006**, *118*, 7836–7878; *Angew. Chem. Int. Ed.* **2006**, *45*, 7674–7715; c) P. Barbaro, C. Bianchini, G. Giambastiani, S. L. Parisel, *Coord. Chem. Rev.* **2004**, *248*, 2131–2150; d) T. J. Colacot, *Chem. Rev.* **2003**, *103*, 3101–3118; e) H.-U. Blaser, *Adv. Synth. Catal.* **2002**, *344*, 17–31; f) G. Bandoli, A. Dolmella, *Coord. Chem. Rev.* **2000**, *209*, 161–196.
[4] M. L. H. Green, D. K. P. Ng, *Chem. Rev.* **1995**, *95*, 439–473.
[5] M. Tamm, *Chem. Commun.* **2008**, 3089–3100.
[6] a) B. Demerseman, P. H. Dixneuf, *J. Organomet. Chem.* **1981**, *210*, C20–C22; b) B. Demerseman, P. H. Dixneuf, J. Douglade, R. Meicier, *Inorg. Chem.* **1982**, *21*, 3942–3947.
[7] a) M. D. Rausch, M. Ogasa, M. A. Ayers, R. D. Rogers, A. N. Rollins, *Organometallics* **1991**, *10*, 2481–2484; b) L. B. Kool, M. Ogasa, M. D. Rausch, R. D. Rogers, *Organometallics* **1989**, *8*, 1785–1790; c) M. Ogasa, M. D. Rausch, R. D. Rogers, *J. Organomet. Chem.* **1991**, *403*, 279–291.
[8] M. Tamm, A. Kunst, T. Bannenberg, E. Herdtweck, P. Sirsch, C. J. Elsevier, J. M. Ernsting, *Angew. Chem.* **2004**, *116*, 5646–5650; *Angew. Chem. Int. Ed.* **2004**, *43*, 5530–5534.
[9] M. Tamm, A. Kunst, T. Bannenberg, E. Herdtweck, R. Schmid, *Organometallics* **2005**, *24*, 3163–3171.
[10] R. J. Baker, T. Bannenberg, A. Kunst, S. Randoll, M. Tamm, *Inorg. Chim. Acta* **2006**, *359*, 4797–4801.
[11] a) M. L. H. Green, N. M. Walker, *J. Chem. Soc. Chem. Commun.* **1989**, 1865–1867; b) G. M. Diamond, M. L. H. Green, P. Mountford, N. M. Walker, J. A. K. Howard, *J. Chem. Soc. Dalton Trans.* **1992**, 417–422.
[12] C. Cornelissen, G. Erker, G. Kehr, R. Fröhlich, *Organometallics* **2005**, *24*, 214–225.
[13] J. C. Flores, R. Hernandez, P. Royo, A. Butt, T. P. Spaniol, J. Okuda, *J. Organomet. Chem.* **2000**, *593*, 202–210.
[14] The Cambridge Structural Database (CSD version 5.29, November 2007) contains 292 structures with 619 Zr–P distances; the distances range from 2.512 to 3.033 Å with a mean value of 2.722 Å.
[15] The Cambridge Structural Database (CSD version 5.29, November 2007) contains 52 structures with 107 Hf–P distances; the distances range from 2.516 to 2.876 Å with a mean value of 2.732 Å.
[16] a) X. D. He, A. Maisonnat, F. Dahan, R. Poilblanc, *Organometallics* **1987**, *6*, 678–680; b) X. D. He, A. Maisonnat, F. Dahan, R. Poilblanc, *Organometallics* **1989**, *8*, 2618–2626; c) M. D. Rausch, W. C. Spink, J. L. Atwood, A. J. Baskar, S. G. Bott, *Organometallics* **1989**, *8*, 2627–2631.
[17] B. Brumas-Soula, F. Dahan, R. Poilblanc, *New J. Chem.* **1998**, *22*, 15–23.
[18] M. S. Blais, R. D. Rogers, M. D. Rausch, *J. Organomet. Chem.* **2000**, *593*, 142–146.
[19] a) G. K. Anderson, M. Lin, M. J. Chiang, *Organometallics* **1990**, *9*, 288–289; b) M. Lin, K. A. Fallis, G. K. Anderson, N. P. Rath, M. Y. Chiang, *J. Am. Chem. Soc.* **1992**, *114*, 4687–4693; c) F. T. Ladipo, G. K. Anderson, N. P. Rath, *Organometallics* **1994**, *13*, 4741–4745.
[20] L. Lettko, M. D. Rausch, *Organometallics* **2000**, *19*, 4060–4065.
[21] R. D. Shannon, *Acta Crystallogr. Sect. A* **1976**, *32*, 751–767.
[22] Y. Zhao, D. G. Truhlar, *Acc. Chem. Res.* **2008**, *41*, 157–167.
[23] D. Holschumacher, T. Bannenberg, C. G. Hrib, P. G. Jones, M. Tamm, *Angew. Chem.* **2008**, *120*, 7538–7542; *Angew. Chem. Int. Ed.* **2008**, *47*, 7428–7432.
[24] We also determined the structure of the isotypic iridium complex: Ir–Cl = 2.3610(5) and Zr–Cl = 2.8265(6) Å; CCDC-711403 contains the supplementary crystallographic data for this paper (these data can be obtained free of charge from The Cambridge Crystallographic Data Centre via www.ccdc.cam.ac.uk/data_request/cif)
[25] B. Cordero, V. Gómez, A. E. Platero-Prats, J. Echeverría, M. Revés, E. Cremades, F. Barragán, S. Alvarez, *Dalton Trans.* **2008**, 2832–2838.
[26] B. E. Bosch, I. Brümmer, K. Kunz, G. Erker, R. Fröhlich, S. Kotila, *Organometallics* **2000**, *19*, 1255–1261.
[27] B. Bosch, G. Erker, R. Fröhlich, *Inorg. Chim. Acta* **1998**, *270*, 446–458.
[28] J. Kuwabara, D. Takeuchi, K. Osakada, *Organometallics* **2004**, *23*, 5092–5095.
[29] G. Mann, C. Incarvito, A. L. Rheingold, J. F. Hartwig, *J. Am. Chem. Soc.* **1999**, *121*, 3224–3225.
[30] G. Menconi, N. Kaltsoyannis, *Organometallics* **2005**, *24*, 1189–1197.
[31] a) L. H. Gade, *Angew. Chem.* **2000**, *112*, 2768–2789; *Angew. Chem. Int. Ed.* **2000**, *39*, 2658–2678; b) N. Wheatley, P. Kalck, *Chem. Rev.* **1999**, *99*, 3379–3419; c) D. W. Stephan, *Coord. Chem. Rev.* **1989**, *95*, 41–107.
[32] For selected references dealing with heterobimetallic complexes supported by cyclopentadienylphosphane ligands, see: a) A. Ricci, F. Angelucci, M. Chiarini, C. Lo Sterzo, D. Masi, G. Giambastiani, C. Bianchini, *Organometallics* **2008**, *27*, 1617–1625; b) L.-C. Song, G.-A. Yu, Y. Liu, B.-S. Yin, X.-G. Zhang, Q.-M. Hu, *Organometallics* **2007**, *26*, 1966–1971; c) C. Cornelißen, G. Erker, G. Kehr, R. Fröhlich, *Dalton Trans.* **2004**, 4059–4063; d) F. Angelucci, A. Ricci, D. Masi, C. Bianchini, C. Lo Sterzo, *Organometallics* **2004**, *23*, 4105–4111; e) F. Angelucci, A. Ricci, C. Lo Sterzo, D. Masi, C. Bianchini, G. Bocelli, *Organometallics* **2002**, *21*, 3001–3008; f) A. Ricci, F. Angelucci, M. Bassetti, C. Lo Sterzo, *J. Am. Chem. Soc.* **2002**, *124*, 1060–1071; g) S. Tollis, V. Narducci, P. Cianfriglia, C. Lo Sterzo, E. Viola, *Organometallics* **1998**, *17*, 2388–2390; h) T. Gutmann, E. Dombrowski, N. Burzlaff, W. A. Schenk, *J. Organomet. Chem.* **1998**, *552*, 91–98; i) P. Cianfriglia, V. Narducci, C. Lo Sterzo, E. Viola, G. Bocelli, T. A. Kodenkandath, *Organometallics* **1996**, *15*, 5220–5230; j) M. J. Doyle, T. J. Duckworth, L. Manojlovic-Muir, M. J. Mays, P. R. Raithby, F. J. Robertson, *J. Chem. Soc. Dalton Trans.* **1992**, 2703–2714; k) C. P. Casey, F. Nief, *Organometallics* **1985**, *4*, 1218–1220; l) C. P. Casey, R. M. Bullock, *Organometallics* **1984**, *3*, 1100–1104; m) C. P. Casey, R. M. Bullock, F. Nief, *J. Am. Chem. Soc.* **1983**, *105*, 7574–7580; n) C. P. Casey, R. M. Bullock, W. C. Fultz, A. L. Rheingold, *Organometallics* **1982**, *1*, 1591–1596; see also refs. [12, 26, 27].
[33] Y. Zhao, D. G. Truhlar, *J. Chem. Phys. A* **2006**, *110*, 5121–5129.
[34] a) M. Kaupp, B. Metz, H. Stoll, *Angew. Chem.* **2000**, *112*, 4780–4782; *Angew. Chem. Int. Ed.* **2000**, *39*, 4607–4609; b) J. Grunenberg, *J. Am. Chem. Soc.* **2004**, *126*, 16310–16311.
[35] Relaxed force constants k (the reciprocal of compliance constants) measure the force required to distort a coordinate by a unit amount while allowing all other coordinates to relax; for details, see: K. Brandhorst, J. Grunenberg, *Chem. Soc. Rev.* **2008**, *37*, 1558–1567.
[36] a) P. D. Harvey, *Coord. Chem. Rev.* **1996**, *153*, 175–198; b) J. R. Lombardi, B. Davis, *Chem. Rev.* **2002**, *102*, 2431–2460.
[37] The Hookean Law ($\Delta E = 1/2k\Delta x^2$) was applied.
[38] This interaction resembles the situation found in unsupported Lewis acid–base adducts between d- and p-block elements, for example, in $[(Cy_3P)_2PtAlCl_3]$ (Cy = cyclohexyl): H. Braunschweig, K. Gruss, K. Radacki, *Angew. Chem.* **2007**, *119*, 7929–7931; *Angew. Chem. Int. Ed.* **2007**, *46*, 7782–7784.
[39] For recent examples, see: a) S. Bontemps, H. Gornitzka, G. Bouhadir, K. Miqueu, D. Bourissou, *Angew. Chem.* **2006**, *118*, 1641–1644; *Angew. Chem. Int. Ed.* **2006**, *45*, 1611–1614; b) M. Sircoglou, S. Bontemps, M. Mercy, N. Saffon, M. Takahashi, G. Bouhadir, L. Maron, D. Bourissou, *Angew. Chem.* **2007**, *119*, 8737–8740; *Angew. Chem. Int. Ed.* **2007**, *46*, 8583–8586; c) S. Bontemps, G. Bouhadir, K. Miqueu, D. Bourissou, *J. Am. Chem. Soc.* **2006**, *128*, 12056–12057; d) S. Bontemps, M. Siroglou, G. Bouhadir, H. Puschmann, J. A. K. Howard, P. W. Dyer, K. Miqueu, D. Bourissou, *Chem. Eur. J.* **2008**, *14*, 731–740; e) S. Bontemps, G. Bouhadir, W. Gu, M. Mercy, C.-H. Chen, B. M. Foxman, L. Maron, O. V. Ozerov, D. Bourissou, *Angew. Chem.* **2008**, *120*, 1503–1506; *Angew. Chem. Int. Ed.*

2008, *47*, 1481–1484; f) M. Siroglou, G. Bouhadir, N. Saffon, K. Miqueu, D. Bourissou, *Organometallics* **2008**, *27*, 1675–1678.
[40] Y. Tatsuno, T. Yoshida, A. Otsuka, *Inorg. Synth.* **1979**, *19*, 220–223.
[41] G. Giordano, R. H. Crabtree, *Inorg. Synth.* **1990**, *28*, 88–90.
[42] Gaussian 03, Revision C.02, M. J. Frisch, G. W. Trucks, H. B. Schlegel, G. E. Scuseria, M. A. Robb, J. R. Cheeseman, J. A. Montgomery, Jr., T. Vreven, K. N. Kudin, J. C. Burant, J. M. Millam, S. S. Iyengar, J. Tomasi, V. Barone, B. Mennucci, M. Cossi, G. Scalmani, N. Rega, G. A. Petersson, H. Nakatsuji, M. Hada, M. Ehara, K. Toyota, R. Fukuda, J. Hasegawa, T. Ishida, M. Nakajima, Y. Honda, O. Kitao, H. Nakai, M. Klene, X. Li, J. E. Knox, H. P. Hratchian, J. B. Cross, V. Bakken, C. Adamo, J. Jaramillo, R. Gomperts, R. E. Stratmann, O. Yazyev, A. J. Austin, R. Cammi, C. Pomelli, J. W. Ochterski, P. Y. Ayala, K. Morokuma, G. A. Voth, P. Salvador, J. J. Dannenberg, V. G. Zakrzewski, S. Dapprich, A. D. Daniels, M. C. Strain, O. Farkas, D. K. Malick, A. D. Rabuck, K. Raghavachari, J. B. Foresman, J. V. Ortiz, Q. Cui, A. G. Baboul, S. Clifford, J. Cioslowski, B. B. Stefanov, G. Liu, A. Liashenko, P. Piskorz, I. Komaromi, R. L. Martin, D. J. Fox, T. Keith, M. A. Al-Laham, C. Y. Peng, A. Nanayakkara, M. Challacombe, P. M. W. Gill, B. Johnson, W. Chen, M. W. Wong, C. Gonzalez, J. A. Pople, Gaussian, Inc., Wallingford, CT, **2004**.
[43] a) A. Bergner, M. Dolg, W. Kuechle, H. Stoll, H. Preuss, *Mol. Phys.* **1993**, *80*, 1431; b) M. Kaupp, P. v. R. Schleyer, H. Stoll, H. Preuss, *J. Chem. Phys.* **1991**, *94*, 1360; c) M. Dolg, H. Stoll, H. Preuss, R. M. Pitzer, *J. Phys. Chem.* **1993**, *97*, 5852.
[44] Details of the variable-temperature NMR study of **10b**/(**10b**)$_2$ and the electronic-structure calculations can be found in the Supporting Information.
[45] G. M. Sheldrick, *Acta Crystallogr. Sect. A* **2007**, *64*, 112–122.

Received: December 2, 2008
Published online: January 14, 2009

